

Hydrodynamics studies of direct-drive cone-in-shell, fast-ignitor targets on OMEGA

C. Stoeckl,¹ T. R. Boehly,¹ J. A. Delettrez,¹ S. P. Hatchett,² J. A. Frenje,³ V. Yu. Glebov,¹ C. K. Li,³ J. E. Miller,¹ R. D. Petrasso,³ F. H. Séguin,³ V. A. Smalyuk,¹ R. B. Stephens,⁴ W. Theobald,¹ B. Yaakobi,¹ and T. C. Sangster¹

¹Laboratory for Laser Energetics, University of Rochester, Rochester, New York 14623, USA

²Lawrence Livermore National Laboratory, Livermore, California 94550, USA

³Plasma Science and Fusion Center, Massachusetts Institute of Technology, Cambridge, Massachusetts 02139, USA

⁴General Atomics, San Diego, California 92121, USA

(Received 22 June 2007; accepted 24 October 2007; published online 28 November 2007)

Experiments have been performed on the OMEGA Laser Facility [T. R. Boehly *et al.*, *Opt. Commun.* **133**, 495 (1997)] to study the hydrodynamics of directly driven cone-in-shell, fast-ignitor targets. A 35° or 70° opening-angle gold cone was inserted into spherical plastic shells of $\sim 24\text{-}\mu\text{m}$ thickness and $\sim 870\text{-}\mu\text{m}$ diameter, which were imploded with up to 21 kJ of 351-nm laser light. A backlighter was used on some experiments to compare the fuel assembly of targets with or without a high-pressure fill gas. The shock breakthrough to the inside of the cone, where the ultrafast laser propagates in integrated fast-ignitor experiments, was studied using a streaked optical pyrometer. No plasma was seen inside the cone before the assembled core reached peak compression. © 2007 American Institute of Physics. [DOI: 10.1063/1.2812706]

I. INTRODUCTION

The reentrant cone-in-shell version^{1,2} of the fast-ignition concept^{3,4} has shown significant promise due to successful integrated experiments.^{5,6} A 1000-fold increase in neutron yield was observed by coupling a 0.5-PW, short-pulse laser into a deuterated plastic (CD) target imploded by 2.5 kJ of laser light at a wavelength of $0.53\ \mu\text{m}$ (Ref. 6). The fast-ignitor concept for inertial confinement fusion (ICF) separates the fuel assembly and fuel heating by combining an ultrafast laser with a driver that compresses the fuel to high density. The ultrafast laser produces relativistic electrons with high efficiency (up to 50% has been reported⁷) that heat the compressed fuel, significantly easing the requirements on the compression driver.^{4,8} Several compression options have been considered, including using laser or heavy-ion beam heated hohlraums or direct laser drive.^{9,10}

The biggest challenge of the fast-ignitor concept is the transport of the relativistic electrons from the critical-density region ($n_e \sim 10^{21}\ \text{cm}^{-3}$ for a typical $1\text{-}\mu\text{m}$ laser), where the ultrafast laser is absorbed and converted into electrons, to the compressed fuel—a distance that can be hundreds of micrometers in an ignition-scale target. The overlap between the electron beam with a divergence of $\sim 40^\circ$ (Refs. 11 and 12) originating from an $\sim 10\text{-}\mu\text{m}$ focal spot and the dense core with a diameter of $< 50\ \mu\text{m}$ would be very small. Two solutions have been proposed to minimize this standoff distance by (i) using a channeling beam to bore a hole in the plasma atmosphere around the core^{4,13,14} and (ii) providing a reentrant cone to allow the laser to propagate as close as possible to the dense core.^{1,2,5}

A few experiments have been performed to assess the potential of the reentrant cone concept. Experiments at the Institute of Laser Engineering (ILE) in Osaka examined the

coupling between the electron beam and the compressed core and found an energy-transfer efficiency of 20–30% (Refs. 5 and 6). Hydrodynamics experiments were performed in both indirect-¹⁵ and direct-drive¹⁶ geometries on OMEGA¹⁷ to study the fuel assembly in the presence of the reentrant cone. The results of these experiments were encouraging, especially for the directly driven configuration. The measured areal densities of the core assembly in the direct-drive experiments are more than 60% of the predicted values for an undisturbed fully spherical implosion,¹⁶ which shows that the core assembly is not considerably disturbed by the presence of the cone. The cone-opening angle was varied from 35° to 70°, with the narrower cones showing a slightly better performance. Significant mixing between the gold cone and plastic shell material was observed in the indirect-drive experiments; this would be detrimental in an ignition design since it substantially increases the required ignition energy.¹⁵ In the direct-drive experiments of Ref. 16, this mixing was reduced to below the detection threshold. Moreover, no filling of the inside of the cone with plasma was observed before peak compression in the direct-drive experiments with 70° cones. The shock driven by the high pressure from the core assembly through the cone material might break out inside the cone and fill it with plasma before the ultrafast laser would be fired, which would significantly increase the standoff between the laser-absorption region and the compressed core.

This work presents hydrodynamics experiments on OMEGA that continue the study of directly driven reentrant cone-in-shell targets. These experiments are in preparation for future integrated experiments on the new OMEGA EP (extended performance) Laser Facility,^{18,19} which will be operational in 2008.

The effect of the presence of gas inside the target on the

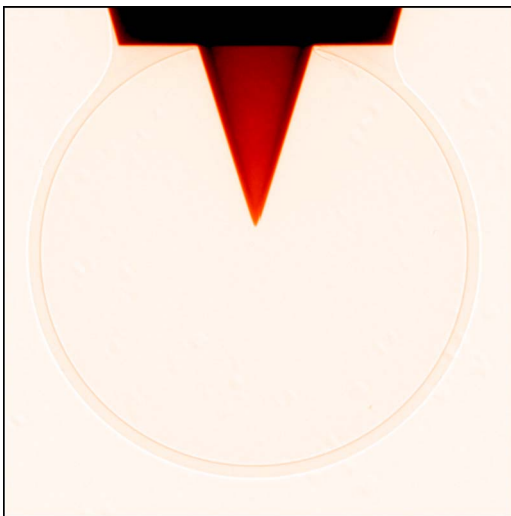


FIG. 1. (Color online) Radiograph of a gas-tight, fast-ignitor cone target. A gold cone with an opening angle of 35° is inserted through a hole in a $24\text{-}\mu\text{m}$ -thick CH shell of $\sim 870\text{-}\mu\text{m}$ outer diameter. A shelf on the cone defines the location of the cone tip at a distance of $30 \pm 10\ \mu\text{m}$ to the center of the shell. It also provides a convenient interface to apply enough glue to make the assembly gas tight.

fuel assembly was studied using backlit implosions of 70° cone targets with or without a high-pressure fill gas. Targets filled with 10 atm of D_2 fuel were used in previous experiments for diagnostic purposes to infer the areal density of the imploded core.¹⁶ The vapor pressure of cryogenic DT²⁰ will also lead to the presence of a fill gas in a full-scale ignition design.²¹ The data from these radiographic experiments were used to confirm the earlier conclusion that there is no significant mixing of gold and core material. The plasma generation inside the cone for 35° cone targets, which showed a better hydrodynamic performance than 70° cone targets in previous experiments,¹⁶ was monitored using a streaked optical pyrometer (SOP).²² The SOP data were used to determine whether the cone stays free of plasma until after the peak areal density of the fuel is reached—the time when the short-pulse beam would be introduced.

Section II describes the experimental setup, including the laser configuration and imaging diagnostic arrangement. Section III discusses the backlighting of the fuel assembly of gas-filled and empty targets and the analysis of the mixing of cone and shell material. Section IV shows measurements of the shock breakout into the inside of the cone. Section V presents the conclusions of this work.

II. EXPERIMENTAL SETUP

The targets used in these experiments were $24\text{-}\mu\text{m}$ -thick CH shells of $\sim 870\text{-}\mu\text{m}$ outer diameter, with a hollow gold cone with an opening angle of 70° or 35° inserted through a hole in the shell (Fig. 1). A shelf on the cone defines the distance between the cone tip and the center of the shell, typically $30 \pm 10\ \mu\text{m}$. It provides a convenient interface for alignment and to make the assembly gas tight. The cone has a thickness of $\sim 100\ \mu\text{m}$ outside the shell and $10\ \mu\text{m}$ inside the shell and ends in a $30\text{-}\mu\text{m}$ -thick hyperbolic-shaped tip with its asymptotes intersecting $12\ \mu\text{m}$ from the target cen-

ter. Two different laser configurations were used to implode these targets on OMEGA: For the backlighting experiments, the target was irradiated using 35 of the 60 OMEGA beams at 351-nm wavelength, with a 1-ns square pulse and $\sim 11\ \text{kJ}$ of laser energy, 15 beams at half energy, and 20 beams at full energy to provide nearly uniform illumination of the shell. All 35 drive beams were smoothed by distributed phase plates (DPP's),²³ two-dimensional smoothing by spectral dispersion (SSD)²⁴ with 1-THz bandwidth in the UV, and polarization smoothing (PS).²⁵ An additional 15 beams with a total energy of $\sim 6\ \text{kJ}$ were diverted to a V backlighter foil and focused to a spot size of $600\ \mu\text{m}$ (no DPP). The axis of this areal backlighting scheme²⁶ was at an angle of $\sim 80^\circ$ from the cone axis, providing a clear view of the core assembly without obscuration from the cone. The cone-filling experiments used 48 beams, with a 1-ns square pulse and $\sim 18\ \text{kJ}$ of total energy (with DPP, SSD, and PS beam smoothing). The laser beams were configured so that no laser light entered the cone. The nearest laser beams irradiated the target at an angle of 59° to the cone axis. The target was supported by a stalk attached to the open end of the cone, to ensure that the target mount did not interfere with any of the laser beams.

X-ray framing cameras²⁷ were used to acquire up to 16 backlit images temporally spaced $\sim 60\ \text{ps}$ apart with an exposure time of $\sim 40\ \text{ps}$ and a spatial resolution of $\sim 10\ \mu\text{m}$ in the target plane. A $25\text{-}\mu\text{m}$ -thick V filter was used to suppress the background radiation from the implosion and pass the predominantly He_α line emission of the V backlighter at $4.95\ \text{keV}$.

The SOP that was used to investigate the filling of the inside of the cone consists of an optical system that images the inside of the tip of the cone onto the slit of the streak camera (see Ref. 16) with an $\sim 10\text{-}\mu\text{m}$ spatial resolution and a $500\text{-}\mu\text{m}$ field of view. The camera is filtered to record in a wavelength band of $660\text{--}850\ \text{nm}$. Various coatings and filters were used to minimize the background from scattered 3ω , 2ω , and 1ω laser light.

III. COMPARISON OF GAS-FILLED AND EMPTY TARGETS

The effect of the gas fill on the core assembly and cone erosion on cone targets with an opening angle of 70° is shown in Fig. 2. Backlit images were recorded using a V backlighter from a target filled with 10 atm of D_2 [Fig. 2(a)] and an empty target [Fig. 2(b)]. Three images, selected out of the 16 images taken, spaced $\sim 250\ \text{ps}$ apart, show the assembly of the core and the erosion of the cone; the central image is close to the time of peak compression. The core assembly, especially the evolution of the core size, is similar in both cases, but the impact on the cone tip is different. In implosions with both empty and gas-filled targets, hot plasma is forced toward the tip of the cone. In the gas-filled case, a larger area at the end of the cone is eroded than with initially empty targets. Self-emission images show similar brightness at the tip of the cone in both cases, so the damage at the cone tip would be comparable in these two cases. The gas-filled target shows less apparent absorption of the backlighter in

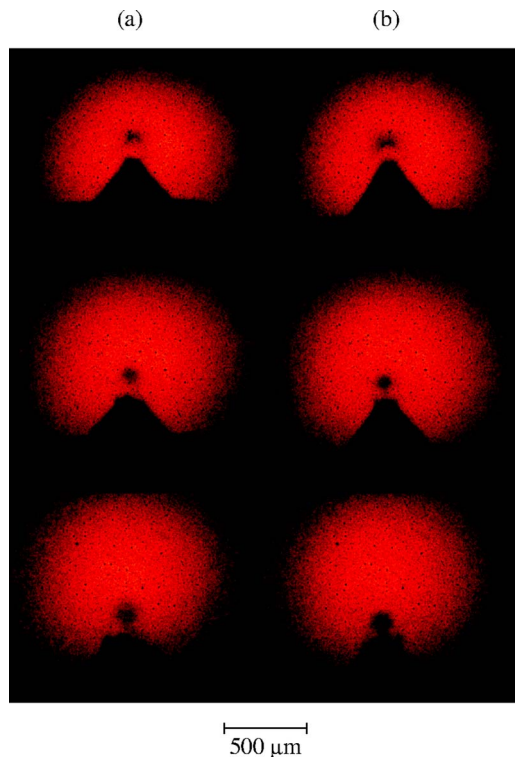


FIG. 2. (Color online) Backlit framing camera images using a V backlighter from 70° cone targets filled with 10 atm of D_2 (a) and without gas fill (b). Three images spaced ~ 250 ps apart show the assembly of the core and the erosion of the cone, with the central image close to the time of peak compression.

the core, probably due to the contribution from the incomplete suppression of the core self-emission.

Figure 3 shows a lineout through the backlit image from an empty target taken at the time of peak compression, i.e., minimum core diameter. The lineout shows the absorption from the cone on the left, a gap in absorption between the cone tip and core, and the absorption from the core assembly. The core shows a slightly asymmetric profile, because plasma streaming toward the cone will be slowed down by the cone plasma, whereas on the other side the core plasma can expand freely. A Gaussian fit to the core absorption, shown in Fig. 3 as a dashed line, makes this asymmetry more noticeable. Beyond this asymmetry caused by the interaction of core and cone plasma (between -60 and $-40 \mu\text{m}$ from the center of the core), no intermixing of Au cone and CH core plasma is observable in this absorption lineout closer than $40 \mu\text{m}$ to the core center. An estimate of the minimum detectable gold contamination in the core can be achieved using a similar analysis as applied to the indirect-drive experiments,¹⁵ where a 0.04%-mass-density gold contamination was inferred. At the plasma conditions expected in the gap—high temperature (>1 keV) and moderate density (<1 g/cm³)—the opacity of CH drops to values of the order of 0.1 g/cm² at the photon energy of the V backlighter of ~ 5 keV. The cold Au opacity of 658 g/cm² can be used because the Au opacity is hardly affected under these conditions. Using these values, a gold contamination of $\sim 0.01\%$ of the mass density in the gap is estimated to cause an $\sim 20\%$

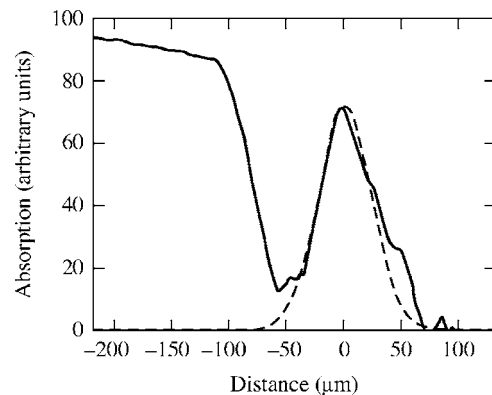


FIG. 3. Lineout through the backlit image from an unfilled target taken at the time of peak compression, i.e., minimum core diameter. A Gaussian fit with a full width at half-maximum of $\sim 70 \mu\text{m}$ to the core absorption is shown as a dashed line.

increase in the expected absorption. No deviation of this magnitude is observed in the symmetry of the absorption from the core shown in Fig. 3 beyond $-40 \mu\text{m}$, which confirms the observation from Ref. 16 that there is very little mixing between cone and core material in these directly driven experiments.

IV. CONE-FILLING STUDIES

The filling of the inside of the cones was investigated using a streaked optical pyrometer (SOP).^{22,28} The breakout of a shock from an opaque material produces a short burst of light. Its timing relative to peak compression can be determined from the absolute temporal calibration of the SOP with an uncertainty of 50 ps. The shock temperature is inferred from the observed light signal using the absolute intensity calibration of the SOP with an uncertainty of 10% at temperatures above ~ 1 eV (Ref. 28). To avoid high background signals in the SOP, either the six laser beams that would illuminate the inside of the cone (23° to the cone axis), or the six 23° beams and the six beams in the vicinity of the cone (48° to the cone axis) were not used in these experiments, ensuring that laser light does not enter the inside of the cone. The SOP looks directly down the axis of the cone, imaging the inside of the cone with a spatial resolution on the order of $\sim 10 \mu\text{m}$ (Ref. 24). Figure 4(a) shows the SOP streak signal from a 35° cone target irradiated by 48 OMEGA beams with a total energy of ~ 18 kJ in a 1-ns square pulse. The vertical axis represents the spatial coordinate of the self-emission from inside the cone, with zero representing the location of the cone tip; the horizontal axis is timed with zero as the start of the laser pulse. Ideally a shock interaction with the cone should produce a signal that begins as a small point at the cone tip and follows the cone-opening angle as the shock travels along the cone. Figure 4 shows this tendency but also has a feature that expands very rapidly in space early in time (2.2–3.0 ns). A ray-trace analysis of the optical system was performed that includes rays reflected from the inner surface of the gold cone. For 35° cones, the light reflected from the cone wall is channeled into the collection optics of the SOP. The fast-evolving feature

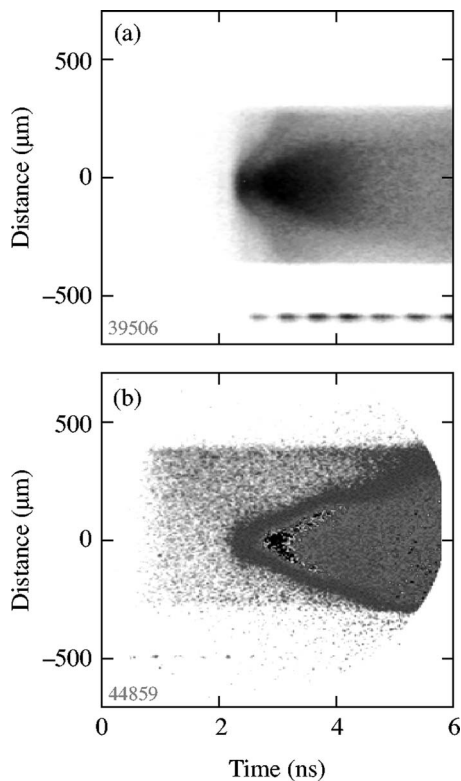


FIG. 4. SOP streak signals from 35° gold cone targets irradiated by 48 (a) or 54 (b) OMEGA beams with a total energy of ~ 21 kJ in a 1-ns square pulse. The time axis zero represents the start of the laser pulse. The signal from an uncoated cone (a) shows a complex structure. A clean shock-breakout signal is seen from (b) a cone coated with black paint on the inside.

seen in Fig. 4(a) early in time is caused by light emitted from the vicinity cone tip, reflected from the cone wall, and recorded by the SOP imaging system as if it originated far away from the cone tip.

To verify this analysis, the inside of a 35° cone was coated with black paint, effectively suppressing the reflections from the cone surface. Figure 4(b) shows the SOP streak signal from such a target irradiated with 54 OMEGA beams with a total energy of ~ 21 kJ in a 1-ns square pulse, which shows a clean shock-breakout signature starting at the tip of the cone, becoming less intense and moving away from the tip as time progresses.

The ray-trace calculations also indicated that 70° cones would not be affected by reflections from the inside of the cone because the reflected rays are not collected by the SOP imaging system. Experiments with 70° cones indeed show a clean shock-breakout signal very similar to Fig. 4(b).¹⁶

Figure 5 shows a lineout through the center of the SOP signal from an uncoated 35° cone target, as well as the areal density of the compressed core as predicted by the 1D hydrocode LILAC²⁹ and the drive laser pulse shape. The calculated time of peak compression from LILAC was found to be within ~ 100 ps from the measured time of smallest core diameter in the time-resolved, framing-camera images shown in Sec. III. Data from an uncoated gold target were used to be able to compare with the published results for the 70° targets.¹⁶ The black paint used to suppress the reflections inside the cone might delay the shock breakout artificially by

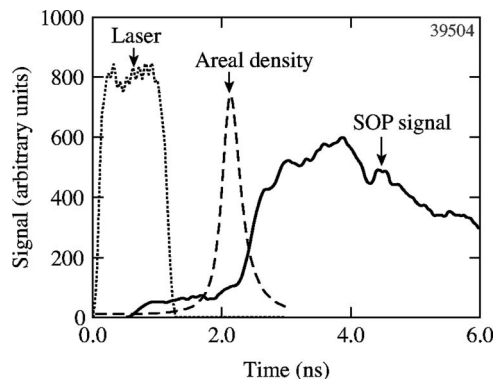


FIG. 5. Lineout through the center of the SOP signal (thick black line) of an uncoated 35° gold cone target. The dotted line shows the laser pulse power and the dashed line represents the calculated evolution of the areal density.

increasing the material thickness. Since this lineout is taken through the center of the SOP signal, it samples only the shock breakout through the cone tip and is not affected by the light reflected inside the cone. The shock signal starts well after (~ 500 ps) the time of peak compression as calculated by LILAC, similar to the earlier results with 70° cone targets.¹⁶ This shows that the inside of the cone is free of plasma at the time when the short-pulse laser would propagate. A shock temperature of the order of ~ 10 eV can be inferred using the absolute intensity calibration of SOP.²⁸

V. CONCLUSIONS

The fuel-assembly experiments with direct-laser-irradiated, cone-in-shell targets presented here show encouraging trends, though significant challenges remain. The mixing of the gold from the cone with the fuel/shell material was confirmed to be very small in these directly driven implosions. With the current cone designs, plasma starts filling the inside of the cone well after peak compression when the ultrafast laser has to propagate through the cone. The observation that the black paint eliminated the reflections inside the cone confirms that the inside surface of the cone stays cold until the shock breaks out at the cone tip.

Gas inside the target, whether added initially or generated during the collapse, could be an issue for fast ignition since it causes erosion of the cone tip. The thickness of the cone tip should also be minimized for experiments with an ultrafast heater beam to limit the energy loss of the relativistic electrons in the gold plasma. The projected range for a 1-MeV electron in room-temperature solid gold is of the order of ~ 50 μm (Ref. 30). Fortunately, in an equivalent cryogenic ignition capsule, the shell and the core would radiate much less energy due to the lower average ionization and the lower drive adiabat.³¹ This will significantly reduce the heating and expansion of the gold cone, its erosion by the core plasma, and the speed of the shock traveling through the cone tip.

ACKNOWLEDGMENTS

The authors are indebted to the Target Fabrication Groups at GA and LLE, especially Mark Bonino, Abbas

Nikroo, and Joe Smith. This work was supported by the U.S. Department of Energy Office of Inertial Confinement Fusion under Cooperative Agreement No. DE-FC52-92SF19460, the University of Rochester, and the New York State Energy Research and Development Authority and with corporate support from General Atomics. The support of DOE does not constitute an endorsement by DOE of the views expressed in this article.

- ¹M. Tabak, E. M. Campbell, J. H. Hammer, W. L. Kruer, M. D. Perry, S. C. Wilks, and J. G. Woodworth, Lawrence Livermore National Laboratory Patent Disclosure, IL-8826B, Lawrence Livermore National Laboratory, Livermore, CA (1997).
- ²P. A. Norreys, R. Allott, R. J. Clarke, J. Collier, D. Neely, S. J. Rose, M. Zepf, M. Santala, A. R. Bell, K. Krushelnick, A. E. Dangor, N. C. Woolsey, R. G. Evans, H. Habara, T. Norimatsu, and R. Kodama, *Phys. Plasmas* **7**, 3721 (2000).
- ³N. G. Basov, S. Yu. Gus'kov, and L. P. Feokistov, *J. Sov. Laser Res.* **13**, 396 (1992).
- ⁴M. Tabak, J. Hammer, M. E. Glinsky, W. L. Kruer, S. C. Wilks, J. Woodworth, E. M. Campbell, M. D. Perry, and R. J. Mason, *Phys. Plasmas* **1**, 1626 (1994).
- ⁵R. Kodama, P. A. Norreys, K. Mima, A. E. Dangor, R. G. Evans, H. Fujita, Y. Kitagawa, K. Krushelnick, T. Miyakoshi, N. Miyanaga, T. Norimatsu, S. J. Rose, T. Shozaki, K. Shigemori, A. Sunahara, M. Tampo, K. A. Tanaka, Y. Toyama, T. Yamanaka, and M. Zepf, *Nature* **412**, 798 (2001).
- ⁶R. Kodama, H. Shiraga, K. Shigemori, Y. Toyama, S. Fujioka, H. Azechi, H. Fujita, H. Habara, T. Hall, Y. Izawa, T. Jitsuno, Y. Kitagawa, K. M. Krushelnick, K. L. Lancaster, K. Mima, K. Nagai, M. Nakai, H. Nishimura, T. Norimatsu, P. A. Norreys, S. Sakabe, K. A. Tanaka, A. Youssef, M. Zepf, and T. Yamanaka, *Nature* **418**, 933 (2002).
- ⁷K. Yasuike, M. H. Key, S. P. Hatchett, R. A. Snavely, and K. B. Wharton, *Rev. Sci. Instrum.* **72**, 1236 (2001).
- ⁸S. Atzeni, *Phys. Plasmas* **6**, 3316 (1999).
- ⁹M. Tabak, D. Hinkel, S. Atzeni, E. M. Campbell, and K. Tanaka, *Fusion Sci. Technol.* **49**, 254 (2006).
- ¹⁰B. G. Logan, R. O. Bangerter, D. A. Callahan, M. Tabak, M. Roth, L. J. Perkins, and G. Caporaso, *Fusion Sci. Technol.* **49**, 399 (2006).
- ¹¹Y. T. Li, J. Zhang, Z. M. Sheng, J. Zheng, Z. L. Chen, R. Kodama, T. Matsuoka, M. Tampo, K. A. Tanaka, T. Tsutsumi, and T. Yabuuchi, *Phys. Rev. E* **69**, 036405 (2004).
- ¹²R. B. Stephens, R. A. Snavely, Y. Aglitskiy, F. Amiranoff, C. Andersen, D. Batani, S. D. Baton, T. Cowan, R. R. Freeman, T. Hall, S. P. Hatchett, J. M. Hill, M. H. Key, J. A. King, J. A. Koch, M. Koenig, A. J. MacKinnon, K. L. Lancaster, E. Martinolli, P. Norreys, E. Perelli-Cippo, M. Rabec Le Gloahec, C. Rousseaux, J. J. Santos, and F. Scianitti, *Phys. Rev. E* **69**, 066414 (2004).
- ¹³Y. Kitagawa, Y. Sentoku, S. Akamatsu, M. Mori, Y. Tohyama, R. Kodama, K. A. Tanaka, H. Fujita, H. Yoshida, S. Matsuo, T. Jitsuno, T. Kawasaki, S. Sakabe, H. Nishimura, Y. Izawa, K. Mima, and T. Yamanaka, *Phys. Plasmas* **9**, 2202 (2002).
- ¹⁴Y. Kitagawa, Y. Sentoku, S. Akamatsu, W. Sakamoto, K. A. Tanaka, R. Kodama, H. Nishimura, Y. Inubushi, M. Nakai, T. Watari, T. Norimatsu, and A. Sunahara, *Phys. Rev. E* **71**, 016403 (2005).
- ¹⁵R. B. Stephens, S. P. Hatchett, R. E. Turner, K. A. Tanaka, and R. Kodama, *Phys. Rev. Lett.* **91**, 185001 (2003).
- ¹⁶C. Stoeckl, T. R. Boehly, J. A. Delettrez, S. P. Hatchett, J. A. Frenje, V. Yu. Glebov, C. K. Li, J. E. Miller, R. D. Petrasso, F. H. Séguin, V. A. Smalyuk, R. B. Stephens, W. Theobald, B. Yaakobi, and T. C. Sangster, *Plasma Phys. Controlled Fusion* **47**, B856 (2005).
- ¹⁷T. R. Boehly, D. L. Brown, R. S. Craxton, R. L. Keck, J. P. Knauer, J. H. Kelly, T. J. Kessler, S. A. Kumpan, S. J. Loucks, S. A. Letzring, F. J. Marshall, R. L. McCrory, S. F. B. Morse, W. Seka, J. M. Soures, and C. P. Verdon, *Opt. Commun.* **133**, 495 (1997).
- ¹⁸C. Stoeckl, J. A. Delettrez, J. H. Kelly, T. J. Kessler, B. E. Kruschwitz, S. J. Loucks, R. L. McCrory, D. D. Meyerhofer, D. N. Maywar, S. F. B. Morse, J. Myatt, A. L. Rigatti, L. J. Waxer, J. D. Zuegel, and R. B. Stephens, *Fusion Sci. Technol.* **49**, 367 (2006).
- ¹⁹L. J. Waxer, V. Bagnoud, I. A. Begishev, M. J. Guardalben, J. Puth, and J. D. Zuegel, *Opt. Lett.* **28**, 1245 (2003).
- ²⁰P. C. Souers, *Hydrogen Properties for Fusion Energy* (University of California Press, Berkeley, 1986).
- ²¹T. C. Sangster, R. Betti, R. S. Craxton, J. A. Delettrez, D. H. Edgell, L. M. Elasky, V. Yu. Glebov, V. N. Goncharov, D. R. Harding, D. Jacobs-Perkins, R. Janezic, R. L. Keck, J. P. Knauer, S. J. Loucks, L. D. Lund, F. J. Marshall, R. L. McCrory, P. W. McKenty, D. D. Meyerhofer, P. B. Radha, S. P. Regan, W. Seka, W. T. Shmayda, S. Skupsky, V. A. Smalyuk, J. M. Soures, C. Stoeckl, B. Yaakobi, J. A. Frenje, C. K. Li, R. D. Petrasso, F. H. Séguin, J. D. Moody, J. A. Atherton, B. D. MacGowan, J. D. Kilkenny, T. P. Bernat, and D. S. Montgomery, *Phys. Plasmas* **14**, 058101 (2007).
- ²²J. A. Oertel, T. J. Murphy, R. R. Berggren, J. Faulkner, R. Schmell, D. Little, T. Archuleta, J. Lopez, J. Verlarde, and R. F. Horton, *Rev. Sci. Instrum.* **70**, 803 (1999).
- ²³Y. Lin, T. J. Kessler, and G. N. Lawrence, *Opt. Lett.* **21**, 1703 (1996).
- ²⁴S. Skupsky and R. S. Craxton, *Phys. Plasmas* **6**, 2157 (1999).
- ²⁵T. R. Boehly, V. A. Smalyuk, D. D. Meyerhofer, J. P. Knauer, D. K. Bradley, R. S. Craxton, M. J. Guardalben, S. Skupsky, and T. J. Kessler, *J. Appl. Phys.* **85**, 3444 (1999).
- ²⁶O. L. Landen, D. R. Farley, S. G. Glendinning, L. M. Logory, P. M. Bell, J. A. Koch, F. D. Lee, D. K. Bradley, D. H. Kalantar, C. A. Back, and R. E. Turner, *Rev. Sci. Instrum.* **72**, 627 (2001).
- ²⁷D. K. Bradley, P. M. Bell, A. K. L. Dymoke-Bradshaw, J. D. Hares, R. E. Bahr, V. A. Smalyuk, D. R. Hargrove, and K. Piston, *Rev. Sci. Instrum.* **72**, 694 (2001).
- ²⁸J. E. Miller, T. R. Boehly, A. Melchior, D. D. Meyerhofer, P. M. Celliers, J. H. Eggert, D. G. Hicks, C. M. Sorce, J. A. Oertel, and P. M. Emmel, *Rev. Sci. Instrum.* **78**, 034903 (2007).
- ²⁹J. Delettrez, R. Epstein, M. C. Richardson, P. A. Jaanimagi, and B. L. Henke, *Phys. Rev. A* **36**, 3926 (1987).
- ³⁰P. K. Gupta, A. K. Kar, M. R. Taghizadeh, and R. G. Harrison, *Appl. Phys. Lett.* **39**, 32 (1981).
- ³¹C. Stoeckl, C. Chiritescu, J. A. Delettrez, R. Epstein, V. Yu. Glebov, D. R. Harding, R. L. Keck, S. J. Loucks, L. D. Lund, R. L. McCrory, P. W. McKenty, F. J. Marshall, D. D. Meyerhofer, S. F. B. Morse, S. P. Regan, P. B. Radha, S. Roberts, T. C. Sangster, W. Seka, S. Skupsky, V. A. Smalyuk, C. Sorce, J. M. Soures, R. P. J. Town, J. A. Frenje, C. K. Li, R. D. Petrasso, F. H. Séguin, K. Fletcher, S. Padalino, C. Freeman, N. Izumi, R. Lerche, and T. W. Phillips, *Phys. Plasmas* **9**, 2195 (2002).